

Large estragole fluxes from oil palms in Borneo

Pawel K. Misztal^{1,2}, Susan M. Owen¹, Alex B. Guenther⁴, Reinhold Rasmussen⁶, Chris Geron⁵, Peter Harley⁴, Gavin J. Phillips¹, Annette Ryan³, David P. Edwards⁷, Nick Hewitt³, Eiko Nemitz¹, Jambery Siong^{8,1}, Mathew R. Heal² and J. Neil Cape¹

[1]{Centre for Ecology & Hydrology, Penicuik, EH26 0QB, UK}

[2]{School of Chemistry, University of Edinburgh, EH9 3JJ, UK}

[3]{Lancaster Environment Centre, Lancaster University, LA1 4YQ, UK}

[4]{Atmospheric Chemistry Division, National Center for Atmospheric Research, 1850 Table Mesa Drive, Boulder Colorado, 80305, USA}

[5]{U.S. Environmental Protection Agency, National Risk Management Research Laboratory, Mail Drop E305-02, 109 TW Alexander Dr., Research Triangle Park, NC 27711, USA}

[6]{Department of Environmental Science and Engineering, Oregon Graduate Institute, P.O. Box 91000, Portland, OR 97291, USA}

[7]{Institute of Integrative and Comparative Biology, University of Leeds, LS2 9JT, UK}

[8] {School of Science and Technology, Universiti Malaysia Sabah, 88999, Malaysia}

Correspondence to: P. K. Misztal (pawel.m@ed.ac.uk)

Keywords: estragole, methyl chavicol, p-allylanisole, 1-allyl-4-methoxybenzene, eddy covariance, ptr-ms, oil palm, *Elaeis guineensis*, weevil, *Elaeiodobius kamerunicus*, tropics, atmospheric chemistry.

Abstract

Estragole (methyl chavicol; IUPAC systematic name 1-allyl-4-methoxybenzene; CAS number 140-67-0) is a known attractant of the African oil palm weevil (*Elaeiodobius kamerunicus*), which pollinates oil palms (*Elaeis guineensis*). The same compound is also commercially available as an insecticide (e.g. against the bark beetle) and is specified as harmful to human health. There has been recent interest in the biogenic emissions of estragole but still it is normally not included in atmospheric models of biogenic emissions and atmospheric

chemistry. We report the first direct canopy-scale measurements of estragole fluxes from tropical oil palms by the virtual disjunct eddy covariance technique. The observed ecosystem mean fluxes and mean ambient volume mixing ratios of estragole are the highest reported so far ($0.49 \text{ mg m}^{-2} \text{ hr}^{-1}$ and 3 ppbv respectively). This may have an impact on regional atmospheric chemistry that previously has not been accounted for in models and could become more important in the future due to expanding oil palm plantations.

1 Introduction

Estragole or 1-allyl-4-methoxybenzene (AMOB) is an oxygenated volatile organic compound (OVOC) with molecular weight of 148 and a boiling point of $216 \text{ }^{\circ}\text{C}$ at atmospheric pressure, sometimes referred to as semi-volatile. Although it is a C-10 compound ($\text{C}_{10}\text{H}_{12}\text{O}$) it is not classified as terpenoid because it is produced by the phenylpropanoid pathway rather than a terpenoid pathway. It has many synonyms, of which the most commonly used after estragole are methyl chavicol, p-allylanisole, isoanethole, chavicyl methyl ether or 1-methoxy-4-prop-2-enylbenzene. Estragole is the original name attributed to the compound and it is used throughout this article. It derives from “estragon”, the French and German word for tarragon (*Artemisia dracunculus*), a herb to which it gives its anis-like odour.

Even though estragole was reported to be a major component of ponderosa pine emissions almost 30 years ago (Altshuller, 1983) a growing interest in this compound in the atmospheric science community has been relatively recent. The interest follows analytical improvements over the last decade which have extended biogenic emission studies to a wider variety of compounds, including estragole. Bouvier-Brown et al. (2009a) recently reported measurements of estragole emissions and ambient concentrations from ponderosa pine trees and highlighted the importance this compound might have for atmospheric chemistry. Lee et al. (2006b) found that the secondary organic aerosol (SOA) yield from full photochemical oxidation of this compound was the highest of all oxygenated terpenes (40%) and also that it was significantly higher than the SOA yield from its ozonolysis (6%) (Lee et al., 2006a). However, estragole is not regarded as an important biogenic VOC (BVOC) for temperate conifer forests (Bouvier-Brown et al., 2009b). Emissions of estragole from oil palms have not yet been quantified even though, as shown later, they exceed many times those reported from other species, and thus their contribution to regional photochemistry is likely to be considerable. Estragole, like many other BVOCs, is suspected to be harmful to human health at high concentrations (EPA, 2002).

Oil palm (Arecaceae *Elaeis*) plantations are an intensively expanding industry in South East Asia. Globally the land area of oil palm plantations is estimated at 13.9 million hectares, where the majority (60%) is concentrated in Malaysia (3.8 Mha) and Indonesia (4.6 Mha) (FAO, 2009). The oil palm cultivated there is usually a high yielding cross between dura and pisifera forms of *Elaeis guineensis* Jacq., which is native to tropical Africa, or hybrids of *E. guineensis* with *E. oleifera*, which is native to Latin America. Plantation area has increased in Malaysia from 55,000 hectares in 1960, to half a million in 1975, and a million hectares were under cultivation in 1980 (Hartley, 1988). Nowadays the area is nearly 4 million ha.

Estragole is the known attractant for the weevil (*Elaeiodobius kamerunicus* Faust) which is the specific pollinator of *Elaeis guineensis* flowers. This weevil responds specifically to estragole and not its derivatives, as was experimentally shown by Hussein et al. (1989). However, for a long time it had been thought that the oil palm is mainly wind pollinated, until Syed (1979) showed in a series of unique experiments that the oil palm is mainly insect pollinated. *Elaeiodobius kamerunicus* is not native to Borneo but was introduced from Cameroon in 1981 for the purpose of improving pollination and increasing crops (Hartley, 1988). The specificity of the pollinator and lack of predators led to a great success for the palm oil industry, saving tens of million pounds on hand pollination (Hussein et al., 1991). Because estragole is also known as an insect deterrent, for example against the bark beetle (e.g. Hayes and Strom, 1994) or fruit flies (Chang et al., 2009), it is therefore possible that this compound may protect the weevil at the oil palm by eliminating their predators. *Elaeiodobius kamerunicus* feeds almost exclusively on oil palm pollen. They are attracted by the aniseed scent of estragole to feed in the male flowers, where pollen grains also stick to their bodies. Female flowers also have an aniseed scent (Mahbob, 2008) so pollen-bearing weevils are also attracted to female inflorescences, thus facilitating pollination. There are two other insects that can have a role in oil palm pollination: *E. subvittatus* and *E. plagiatus* (Moura et al., 2008) but they have not yet been introduced to Borneo. In addition, in peninsular Malaysia (but not in Borneo) *Thrips hawaiiensis* and *Pyroderces* sp. may also possibly play a role in pollination of the oil palm (Wahid and Kamarudin, 1997)

The lifetime of estragole in the atmosphere has been estimated for temperate latitudes by Bouvier-Brown et al. (2009a) as 55 min and 18 h for reaction with OH and O₃, respectively, suggesting that this compound can have an impact on regional photochemistry. Estragole

oxidation is not included in the Master Chemical Mechanism (MCM)¹, nor are any other aromatic species with methoxy or 2-propenyl substituents. The reactivity of estragole to OH might be expected to be similar to that of methoxybenzene, or the methoxy-substituted aromatic ring ($\sim 3 \times 10^{-11} \text{ cm}^3 \text{ molecule}^{-1} \text{ s}^{-1}$) and that the side chain would react similarly to a terminal alkene (M.E. Jenkin, personal communication). Recently, Bouvier-Brown et al. (2009a) reported two consistent estimates for k_{OH} of $5.7 \times 10^{-11} \text{ cm}^3 \text{ molecule}^{-1} \text{ s}^{-1}$ from ozonolysis studies performed by Lee et al. (2006a;2006b) and $5.4 \times 10^{-11} \text{ cm}^3 \text{ molecule}^{-1} \text{ s}^{-1}$ derived using the Environmental Protection Agency's Estimation Program Interface Suite (EPA, 2000). These are similar to the k_{OH} value for 2-methyl-3-buten-2-ol (MBO). The same authors also estimated rate coefficients for the reaction of estragole with ozone (k_{O_3}) of $1.4 \times 10^{-17} \text{ cm}^3 \text{ molecule}^{-1} \text{ s}^{-1}$ and $1.2 \times 10^{-17} \text{ cm}^3 \text{ molecule}^{-1} \text{ s}^{-1}$ from the same two approaches. It would be anticipated that the initial stages of estragole degradation are efficient at generating ozone, since 1-alkenes typically have photochemical ozone creation potentials (POCP) of around 100. On the other hand, if degradation leads to compounds of similar structures to benzaldehyde or nitrophenols, then impact on ozone formation will be near zero or negative since these compounds lead to near-irreversible sequestration of NO_x and organic material into species which deposit efficiently or are incorporated into aerosol. But in that case, estragole would be expected to act as an efficient SOA precursor (M.E. Jenkin). In both cases estragole oxidation will likely have impact on regional photochemistry.

In May and June 2008 measurements of VOC fluxes by virtual disjunct eddy covariance (continuous flow disjunct) were made using proton transfer reaction mass spectroscopy (PTR-MS), and were supplemented by GC-MS study (leaf level and ambient) at an oil palm plantation in Sabah, Borneo². Estragole was the second most abundant BVOC (after isoprene) at the plantation and the observed concentration and fluxes are the highest reported so far from vegetation.

¹ <http://mcm.leeds.ac.uk/MCM/>

² Misztal, P. K., Nemitz, E., Langford, B., Coyle, M., Ryder, J., DiMarco, C., Phillips, G., Oram, D., Owen, S., Heal, M. R. and Cape, J. N.: First direct ecosystem fluxes of VOCs from oil palms in SE Asia, Atmos. Chem. Phys. Discuss., in preparation for submission, 2009

2 Methods

2.1 Site and setup

The experiment site was a flat 33 ha commercial oil palm plantation located at 5°14'52.67 (N) latitude and 118°27'14.96 (E) longitude within a much larger oil palm area belonging to the Sabahmas Oil Palm Plantation owned by Wilmar International Ltd. (Figure 1). This location is 28 km NE of Lahad Datu in the Malaysian province of Sabah in NE Borneo. The palms were 12 year old *E. guineensis* × *E. oleifera* hybrids of the progeny “Gutherie”, with an average height of 12 m and a single-sided leaf area index (LAI) of about 6, planted at a commercial density of 150 trees per ha. The suite of atmospheric measurements at this site and a rainforest site during OP3 and ACES measurement campaigns is summarised in the introductory paper of this issue (Hewitt et al., 2009)

2.2 Proton Transfer Reaction Mass Spectrometer (PTR-MS)

A Proton Transfer Reaction Mass Spectrometer (PTR-MS) was employed to monitor the VOC concentrations and eddy fluxes of various compounds including estragole. The PTR-MS instrument was a high sensitivity model (Ionicon Innsbruck, Austria, s/n: 04-03) incorporating an additional turbopump for the detection chamber and Teflon instead of Viton rings in the drift tube. In addition in our instrument the Pfeiffer turbopumps have been replaced with their Varian analogues. Operational details have been described elsewhere (e.g. de Gouw et al., 2003;Lindinger et al., 1998), and very recently the PTR-MS technique has been reviewed by Blake et al.(2009), hence only a brief description is presented here. The VOCs under study, whose proton affinities exceed that of water, are soft-ionised in a drift tube by collision with hydronium ions, formed in the hollow cathode of the ion source. The products of the proton transfer reactions are either protonated compounds or their protonated fragments or clusters. The magnitude of fragmentation/clustering can be optimised by adjusting the electric field (E) and the buffer gas number density (N) in the drift tube, so that the E/N ratio is most commonly in the range of 120-140 Td (1 Td = 10^{-17} V cm²). The relative abundance of the product cations, separated by the quadrupole mass filter, can be derived from the number of pulses counted by the Secondary Electron Multiplier (SEM) during a given dwell time. During the PTR-MS measurements at the plantation the E/N ratio was kept constant at 140 Td

by adjusting drift tube parameters of pressure to 160 Pa, temperature to 45 °C and the drift voltage to 485 V. The sampling inlet and the 20 Hz sonic anemometer (Solent R3, Gill Instruments) were placed above the canopy at about 15 m. A 20 m PTFE sampling line (1/4'' OD, 3/16'' ID) was used to draw a flow rate of 35 L min⁻¹ past the instrument, which sub-sampled at a flow rate of 400 mL min⁻¹. The instrument and PTFE tubing were protected against water condensation by heating above the ambient temperature (approx. 50 °C) using a heating tape. In order to get absolute volume mixing ratios, either calibration with an external standard is required, or less precise calculation can be made based on the calibrated transmission of the instrument and the proton transfer reaction rate of estragole. As no estragole calibration standard was available for PTR-MS at the site, the instrument was calibrated against several other VOCs (i.e. methanol, acetonitrile, acetone, acetaldehyde, isoprene, a monoterpene: d-limonene) and then the relative transmission curve was obtained to yield an empirical calibration coefficient for estragole (method described by Taipale et al., (2008)).

The biggest advantage of PTR-MS is the high frequency of data acquisition, which makes it suitable for use in micrometeorological flux measurement techniques such as eddy covariance (EC). Here, data were processed according to the virtual disjunct eddy covariance concept (Karl et al., 2002; Rinne, 2001), where for each m/z of interest the PTR-MS makes a measurement which is sufficiently fast (as determined by the dwell time), but discontinuous (while the PTR-MS scans the other m/z of interest), thus providing fewer data points than continuous EC. The effective time lag associated with the residence time in the tubing was calculated from the cross-correlation between vertical wind speed and the VOC mixing ratio as a function of lag time (Davison et al., 2009; Langford et al., 2009; Rinne et al., 2007; Spirig et al., 2005). If no true peak was present in the covariance function or if it was smaller than the detection limit derived by multiplying the standard deviation of the noise over 180 s by 1.5, then the flux data point was discarded. In addition the data were filtered for stationarity using the criterion of Foken and Wichura (1996) and for low friction velocity ($u_* < 0.15 \text{ m s}^{-1}$).

Estragole is detected at m/z 149 in PTR-MS as the protonated molecular ion. It was measured for the first time with PTR-MS in ambient air by Holzinger et al. (2005). This compound is relatively resistant to fragmentation at typical working conditions, with only small fragmentation to m/z 121, and thus PTR-MS can be used reliably for monitoring its

concentrations and fluxes. There are only a few minor contributions to m/z 149 known from other compounds that have been reported so far, of which the most significant are from sesquiterpenes (Bouvier-Brown et al., 2007; Bouvier-Brown et al., 2009b; Helmig et al., 2006; Kim et al., 2008). When the volume mixing ratio of sesquiterpenes relative to estragole is very low, one can assume these contributions to be insignificant. In addition, a GC-MS was used to check the ambient air for any interference with the m/z 149 signal. Fluxes of other compounds measured with the PTR-MS at the oil palm plantation included isoprene, total monoterpenes and methanol. These results are presented in a separate paper (Misztal et al., 2009)³.

2.3 Gas chromatography (GC-MS)

2.3.1 Leaf cuvette sampling method

Two types of leaf cuvette were used for sampling VOC emissions, an ADC LCpro (ADC Bioscientific Ltd. UK), and a Li-Cor Li-6400 (Li-Cor, Inc., Lincoln, Nebraska, USA). Both types of cuvette are portable photosynthesis systems, measuring water vapour (H₂O) and carbon dioxide (CO₂) exchange from the leaf surfaces with infrared gas analyzers (IRGAs) and allowing control of photosynthetic photon flux density (PPFD), leaf and air temperature, humidity, CO₂ concentration, and airflow rate. They were adapted for sampling VOC emissions by introducing a sampling port in the gas line exiting the cuvette.

Before each measurement campaign, the leaf cuvettes had been serviced and checked, and were in optimal working order. A charcoal filter was fitted to the inflow of the leaf cuvettes to remove ambient BVOCs and ozone. This had the effect of elevating the ambient CO₂ concentrations by about 50 ppm on average in the LCpro, but this was fairly consistent for all emission samples. While this is a little higher than the average ambient [CO₂], there are several reports of high [CO₂] between 1 and 5 m from a tropical forest floor during the morning and later in the afternoon (e.g. Buchmann et al., 1997; Culf et al., 1999). Rosenstiel et al. (2003) found that increasing CO₂ concentrations reduces canopy isoprene emission and decouples isoprene emissions from photosynthesis; however, they worked with concentrations of 800 and 1200 ppm, which is far higher than the concentrations the sampled leaves

³ Misztal, P. K., Nemitz, E., Langford, B., Coyle, M., Ryder, J., DiMarco, C., Phillips, G., Oram, D., Owen, S., and Cape, J. N.: First direct ecosystem fluxes of VOCs from oil palms in SE Asia. *Atmos. Chem. Phys. Discuss.*, in preparation for submission 2009

experienced in the investigation reported here (400 ppm). Using a charcoal trap to clean inflowing air might result in upper-limit emission measurements because purified air can result in a higher concentration gradient of emitted compound between leaf air space and ambient air. But in nature, wind or high ozone concentrations reacting with emitted products would also increase monoterpene concentration gradients. We consider that natural factors affecting concentration gradients of emitted compounds are complex and variable, and assume that concentration gradients of emitted compounds resulting from using a charcoal filter are likely to be matched in nature with reasonable frequency.

Inter-comparison experiments performed during previous studies showed that BVOC emissions measured using the ADC LCpro cuvette system were comparable with those measured using the Li-COR system (Geron et al., 2006). The leaf cuvettes were installed on a leaf and left to equilibrate for 45 min before VOC samples were taken. Flow rate through the ADC LCpro was 300 mL min⁻¹, and 500 mL min⁻¹ through the Li-COR. Sampled leaf areas in the ADC LCpro and Li-COR were 6.25 cm² and 6 cm², respectively. Photosynthetically active radiation (PAR) in the leaf cuvettes was set at an optimum (i.e. 500 μmol m² s⁻¹ for plants under the canopy; 1000 μmol m² s⁻¹ for plants that are exposed to sunlight). Carbon dioxide and humidity were both set to ambient conditions to simulate the plant's actual field condition. Leaf temperature was set at 30 °C or slightly higher to minimise condensation in the cuvettes.

Samples were analyzed by three independent methods including an in-situ portable GCMS, collection in stainless steel canisters transported to laboratory for analysis, and collection on solid adsorbent cartridges transported to laboratory for analysis. Sample cartridges were filled with 100 mg Carbotrap and 200 mg Tenax and conditioned for 15 min at 300 °C in a flow of helium. Cartridges prepared in this way have been used in our laboratory for many years, and are always very consistent in their adsorbent properties. A cartridge was fitted to the cuvette outlet port, and air from the cuvette drawn through it at 100–120 mL min⁻¹ using an SFK mass flow controlled pocket sampling pump. This range of flow rates ensured that only cuvette air was sampled, and was not contaminated with outside air. Samples were taken for 10–20 min, and the cartridges were stored in a refrigerator until returned to CEH, Edinburgh, UK, for analysis using gas chromatography with mass selective detection (GC-MS). In a previous study using the same sampling and analytical system, changes in sample compound content were assessed during storage and transport. Overall, there was between 0.1% and 10.4% more

of each compound in the transported standard tubes compared with freshly injected standards, but differences were not significant, due to variability in different batches of diluted standards (Wang et al., 2007). In addition, a sample was taken from an empty leaf cuvette each day to give a blank value which was subtracted from emission samples.

2.3.2 GC-MS analysis

Leaf samples were analysed using a GC-MS system. A thermal desorption autosampler (Perkin-Elmer ATD 400) was connected via a heated (200 °C) transfer line to a Hewlett-Packard 5890 GC with a 5970 mass-selective detector.

Compounds were desorbed at 280 °C for 5 min at 25 mL min⁻¹ onto a Tenax-TA cold trap maintained at -30°C. Secondary desorption was at 300 °C for 6 min onto the GC column. Separation of the compounds was achieved using an Ultra-2 column, Agilent Technologies (50 m x 0.2 mm x 0.11 µm ID, 5% phenylmethyl silica). The initial oven temperature of 35 °C was maintained for 2 min, then increased at 4 °C min⁻¹ to 160 °C followed by an increase of 45 °C min⁻¹ to 300 °C which was maintained for 10 min. The carrier gas was helium at ~1 mL min⁻¹, the injector temperature was 250 °C. For this system, the limit of detection for isoprene and monoterpenes was approximately 0.25 and 2 ng on column for isoprene and monoterpenes, and sesquiterpenes, respectively, corresponding to 100 and 50 pptv of isoprene and monoterpenes in air for a 1 L sample, and 400 pptv of sesquiterpenes in a 1 L sample. The level of analytical precision was around 6.5% for isoprene, 5% for monoterpenes and 10% for sesquiterpenes.

Monoterpene quantification was by comparison with commercially available liquid standards (Aldrich, Fluka and Sigma) appropriately diluted in solution before injecting on column and isoprene quantification by comparison with a 1 ppmV in N₂ certified gas standard (Air Products UK). Chemstation for Microsoft Windows was used to handle chromatographic data. Identification was achieved by comparison of retention times and mass spectra of authentic standards. Samples were analysed in "scan" mode, but subsequent quantification was achieved by standard calibration and integration of selected ion spectra for isoprene (*m/z* 67) and monoterpenes (*m/z* 93). Ions for identification of estragole were at *m/z* 148, 147, 77, 121, and 117 and the estragole peak appeared at retention time 28.15 mins. There was no standard available for estragole, so it was quantified by comparing the response of *m/z* 77 with that of the α -pinene standard.

Ambient air and enclosure samples were also analyzed in-situ with a portable gas chromatograph with a mass spectrometer (Hapsite Smart, Inficon, East Syracuse NY). using a 30 m x 0.32 mm ID 1 mm film DB-1 column, temperature programmed with an initial 2 min hold at 40 °C followed by a 15 °C min⁻¹ ramp to 80 °C followed by a 3 °C min⁻¹ ramp to 110 °C followed by a 9 °C min⁻¹ ramp to 200 °C with a final 6 min hold. VOCs were quantified with respect to an internal standard referenced to NIST traceable standards.

2.4 TOF-AMS

An Aerodyne high-resolution time-of-flight aerosol mass spectrometer (HR-ToF-AMS) was used to monitor the composition of non-refractory sub-micron PM at the oil palm plantation. The HR-ToF-AMS has been described in detail in DiCarlo et al., (2006) and is a further development of the original Aerodyne quadrupole aerosol mass spectrometer (Jayne et al., 2000; Jimenez et al., 2003). The ambient air was sampled down a 15 m ¼” stainless steel inlet tube and sub-sampled by the AMS via a Nafion drier. The inlet was situated next to the sonic anemometer just above the oil palm canopy co-located with the PTR-MS. The AMS uses an aerodynamic lens in a differentially-pumped vacuum chamber to enhance the aerosol mass over the gas in the sample. The aerosol was vaporised at 600 °C and extracted into the ToF mass spectrometer.

The instrument was operated in the general alternation mode, switching between the MS/PToF mode and the high resolution MS modes every 5 min every other half hour. The remaining half hour was used for eddy-covariance flux measurements not presented in this paper. The data analysis was performed using SQUIRREL, the standard ToF-AMS analysis suite developed by the Universities of Manchester and Colorado and Aerodyne Research and hosted electronically at the University of Colorado at Boulder⁴. Here only parts of the dataset are used, with a more detailed analysis of the aerosol composition and fluxes provided by Nemitz et al. (2009)⁵.

⁴ <http://cires.colorado.edu/jimenez-group/ToFAMSResources/ToFSoftware/index.html>

⁵ Nemitz et al. 2009, in preparation for Atmos. Chem. Phys. Discuss., 2009.

3 Results and discussion

3.1 Estragole mixing ratios

3.1.1 Specificity for oil palm and screening for anisoles

Estragole, being p-allyl-anisole, belongs to the family of anisole compounds whose structure includes a methoxy group attached to a benzene ring. Emission of aromatic compounds from vegetation, although very interesting biochemically, is still not well represented in published data, but includes reports of biogenic emissions of typical anthropogenic compounds like toluene (Heiden et al., 1999). During measurements in Borneo estragole was only found at the oil palm plantation, and it was not detected either above a rainforest canopy or in the screening of individual tree foliage in a jungle. In fact, in the rainforest, anisole and many of its derivatives (e.g. p-vinyl-anisole, p-ethyl-anisole, p-ethylene-anisole) were detected lower in the canopy by PTR-MS, but not p-allyl-anisole (estragole) either below or above canopy. An example chromatogram of this screening at the forest, presenting several anisole species emitted from the surface of an old fig tree leaf, is shown in Figure 2. The leaf had a spicy anise fragrance. It was held in the dark, so there was very little isoprene. Heavy algal/fungal growth was present on the leaf surface. These chemical compounds were relatively low in abundance and they were often associated with phyllosphere organisms and therefore could possibly play a role in defence mechanisms or be a microbial product.

Comment [PKM1]: Rei: how would be best to crossreference with your findings?

By comparison, in the oil palm ambient air, estragole, but none of its derivatives, was the second most abundant measured VOC after isoprene. In Figure 3 the chromatogram of oil palm ambient air is shown, analogous to the one presented in Figure 2, revealing the peak of estragole dominating the signal. The isoprene peak is at ?? min and is not shown. It is worth noting that the high abundance of estragole in the ambient air above the oil palm canopy was recorded by both PTR-MS and GC-MS, while the leaf-cuvette study detected only very small concentrations of estragole and in only a few percent of the samples. This clearly indicates that estragole is not primarily emitted by the fronds, but almost certainly is released by the flowers, which is not surprising, bearing in mind its role in pollination. As leaf surfaces can adsorb and store significant amounts of deposited gases (Binnie et al., 2002) it is likely that small emissions from fronds are secondary to previous deposition, which was quite frequent for this semi-volatile compound. Due to the fact that sampling was not directly from the flowers, one might argue about possibly different sources (e.g. fruit, stems, etc.).

Comment [PKM2]: Rei: would you please have this info?

Nevertheless, estragole has an intense aniseed scent and from observation of the weevil's role in pollination it seems apparent that it is attracted to the flower (Mahbob, 2008). Neither fruit nor leaves had an obvious smell of aniseed. See Section 3.3 (below).

3.1.2 Diurnal cycles

Results from the leaf emission samples and random ambient air samples for analysis by GC-MS are presented in Table 1. The time series for estragole mixing ratios recorded by PTR-MS is shown in Figure 4 and the diurnal average is presented in Figure 5a in comparison with temperature and PAR. In addition, the Box-and-Whisker plot in Figure 5b illustrates its day-to-day variability. As most insects avoid tropical heat, the synergy of estragole maximal release with the likely feeding/pollinating time of the insect can be seen in the estragole diurnal cycles, which moderately correlate with temperature corrected by a lag of ~3.5 h, suggesting a short-term storage pool in the plant before release a few hours later.

The estragole mixing ratio from PTR-MS was moderately correlated with the 3.5 h lag-adjusted temperature ($r^2 = 0.4$) and the 4.5 h lag-adjusted PAR ($r^2 = 0.34$), but without a lag correction no correlations were found. This is different from the case of other VOCs, whose responses to temperature (or PAR) were almost instantaneous. Based on the mass scan (m/z 21-205) performed on the PTR-MS every hour the highest correlations between estragole normalised signal at m/z 149 were found with m/z 95 ($r^2 = 0.38$), m/z 75 ($r^2 = 0.33$), m/z 47 ($r^2 = 0.30$) and m/z 121 ($r^2 = 0.24$), which could be due to internal fragmentation. There were also weak correlations with some other biogenic masses ($r^2 < 0.2$).

It is common for some fragmenting compounds (e.g. isoprene) to deviate from the relative transmission curve but it was assumed that fragmentation of estragole was not significant. The uncertainty of such empirical sensitivity approach lies between the error of calibration with a standard (typically 5-10%) and the error of deriving the mixing ratios from drift tube reaction kinetics and proton transfer reaction rate constants (up to 100%) (e.g. Steinbacher et al., 2004).

3.2 Estragole fluxes

Previous PTR-MS measurements over pines (Bouvier-Brown et al., 2009a; Bouvier-Brown et al., 2009b; Holzinger et al., 2005) showed concentrations of 2-methyl-3-butenol (MBO) to correlate closely with estragole. However, at the oil palm plantation MBO was not observed, which highlights a different biochemistry of conifer and floral emissions, or might be dependent on the species. Therefore the method suggested by Bouvier-Brown et al. (2009a) of inferring estragole emissions from correlation with MBO is not applicable for oil palm. A comparison of fluxes reported from other environments is shown in Table 2. It is worth emphasizing that the observed fluxes above oil palms are the highest reported so far, and for the first time reported from tropical oil palms. The flux time series is presented in Figure 6a which shows periods of correlation and anti-correlation with sensible-heat flux (Figure 6b), which was not always strong. This can be explained in part by periods of estragole deposition, delayed temperature response and local gradients caused by possibly slightly different release times of particular inflorescences. Night time emission and deposition are uncertain as the flux was generally below the detection limit and the turbulence was insufficient (small u^*). However, the low estragole concentrations observed in the shallow night-time boundary layer confirm that night-time emissions are very low. The highest fluxes were normally observed during the middle of the day, peaking at approximately $2 \text{ mg m}^{-2} \text{ h}^{-1}$. There were also periods of apparent deposition for estragole. On the averaged diurnal graph (Figure 7b) one can see the estragole flux in comparison with the sensible heat flux and friction velocity (on the colour scale). Although in the mixing ratios there was a delayed correlation observed with temperature, it seems that there is not a large shift in the flux compared with the sensible heat flux. This is because most of the eddy flux is driven by turbulence, and thus as soon as mixing within the PBL decreases it appears that there is an accumulation of estragole, which slowly decays overnight. It would be interesting to study if estragole can be taken up by palms during the night, whether it can penetrate into the soil, and to better understand its ventilation and chemistry at night. The Box-and-Whisker plot in Figure 7b shows high day-to-day variability, probably due to periods of deposition but also because the strength of the particular flower sources operating in a 5 day pollination cycle can be varied as more flowers, on the spikelets /inflorescences, are becoming active/inactive.

3.3 Contribution of estragole from oil palms to global emissions

The 24-hour average canopy flux of estragole for the period 29/05 – 11/06/2008 (12 days of measurement) including both emission and deposition amounts for $0.24 \text{ mg m}^{-2} \text{ h}^{-1}$. Assuming the total area of oil palm plantations worldwide of 13.9 million hectares, the up-scale of this flux would yield the value of 292 Gg (10^9) of globally emitted estragole per year (365.25 days), with the regional 60% contribution for Indonesia and Malaysia region of 175 Gg yr^{-1} . This is a very large flux in terms of regional contribution, and probably the highest global floral emission source, which is three order of magnitudes lower than estimates of global isoprene emission.

3.4 Investigating emissions of estragole from male and female inflorescences of Oil Palm

A semi-quantitative approach was used to confirm that oil palm flowers are indeed the source of estragole in the atmosphere above oil palm plantations. Six different inflorescences which were typical in appearance and health (based on visual inspection) were randomly selected within a commercial oil palm plantation. Three inflorescences were male, and three were female. They were enclosed, in turn, in wide transparent Teflon bags, which were open at both ends. The bags were secured gently around the base of the inflorescence with a cable tie. The other end of the Teflon bag was also closed with a cable tie around the whole inflorescence, leaving enough of a gap to insert a stainless steel sample tube (6 mm o.d.) filled with Tenax and Carbotrap (as above). The system was static, and after installation, it was left for an hour to allow any compounds emitted from the flowers to accumulate inside the Teflon enclosure. A sample tube was then inserted into the small gap left at the closed end. The sample tube was attached to a pump and sampled at a rate of 150 mL min^{-1} for 15 minutes, giving a total sample volume of 2.25 L. During sampling, it was inevitable that air flowed into the Teflon enclosure from outside via the gap around the base of the inflorescence, but the total bag volume was $\sim 8 \text{ L}$, so the dilution effect would have been at most $\sim 30\%$.

Female inflorescences yielded estragole concentrations in the sample tubes ranging from $0.31 - 1.69 \text{ } \mu\text{g L}^{-1}$. This corresponds to an accumulated concentration over an hour ranging from $\sim 0.26 - 1.39 \text{ ppm}$. Concentrations were higher in the morning than later in the day. However, the third female inflorescence gave sample concentrations which were in excess of $77 \text{ } \mu\text{g L}^{-1}$ in the morning ($\sim 60 \text{ ppm}$). It is possible that the sample tubes for this female flower actually

touched the source of estragole in the inflorescence, and contaminated the steel case. In contrast, male inflorescences gave lower concentrations in the sample tubes ranging from 0.02 – 0.18 $\mu\text{g L}^{-1}$ (up to ~ 0.15 ppm). Concentrations tended to be higher in the middle part of the day. Generally, male and female inflorescences weigh about 0.5 kg and 1 kg, respectively. Therefore differences in mass do not entirely account for the different concentrations found in samples from male and female inflorescences. Because the concentrations in the samples saturated the GC-MS detector, these estimates under-estimate the true concentrations by an unknown factor.

Although it is not possible to report accurate quantitative fluxes of estragole from oil palm flowers, if an average of 15 female inflorescences per tree is assumed, and a planting density of 150 trees ha^{-1} , one derives a semi-quantitative estimate of up to 0.03 $\text{mg m}^{-2} \text{h}^{-1}$ emission of estragole from female flowers. This is an order of magnitude lower than the flux values derived from the PTR-MS, and is partly attributable to the GC-MS detector saturation, and likely dilution with inflowing ambient air into the static sampling chamber. Nevertheless, the high concentrations up to 60 ppm accumulated in the bag show conclusively that oil palm flowers are a significant source of estragole in the atmosphere above oil palm plantations, although the possibility of another source within the plantation biota cannot be excluded.

3.5 Dependence on wind direction and relative humidity

A polar plot of wind speed vs. wind direction (Figure 8a) shows highest wind speeds from SSE and ESE, while moderate wind speed seems to be evenly distributed. The strongest winds could theoretically have been advecting polluted air from a residential area about 300 m E of the site, but not from a palm oil processing mill about 8 km W. In addition, the hourly mass spectrum scans did not show any elevated signal at m/z 79, typically attributed to benzene (anthropogenic pollution marker) and winds were generally not strong. The polar plot and probability wind rose for estragole mixing ratios are presented in Figure 8b and Figure 8c, showing the highest probability of contributions from the S, SW and SE. In addition the former graph has been coloured in relation to relative humidity. It seems that the most humid air ($\text{RH} > 90\%$) was coming mainly from S and N while less humid air ($60\% < \text{RH} < 75\%$) was mainly from E and W. Humidity did not have a strong correlation with the estragole mixing ratios although the smallest values were centred around the highest RH. Similarly, the polar plots for the fluxes are shown in Figure 9(a-c), with emission and deposition presented separately on the same graph (Figure 9a). Because the oil palm

vegetation was clearly homogeneous, the sources and sinks should be similarly distributed. Again, the polar plot for estragole emission (Figure 9b) has been coloured according to relative humidity. This typically shows the smallest flux at the highest RH and the higher fluxes were observed when air was not completely saturated with water vapour, the former possibly attributed to “wash-out” effect due to greater losses in wet deposition of VOCs . Finally the probability wind rose for estragole emissions is presented in Figure 9c, showing their distribution skewed towards S, SW, and SE, which can be linked with higher wind frequencies occurring at those directions and which are fairly consistent with the probability plot for estragole mixing ratios based on more data points.

3.6 Estragole partitioning in the aerosol phase

Estragole has a relatively high aerosol partition coefficient, $\log K_{oa}$ octanol-air partition coefficient estimated by KOAWINTM v1.10 (EPA, 2007a) at 5.194, and in certain conditions can partition into the aerosol phase. In Figure10 the comparison between estragole in the aerosol phase (estimated from the sum of fragments at m/z 53, 70, 77, 91, 115, 147 on the TOF-AMS) and gaseous fraction are presented. The morning peak, related to a rise in aerosol fraction, can be seen on particular days by AMS and the late peak is generally dominated by PTR-MS. This behaviour seems to be reasonable for an effective pollinator attractor.

3.7 Parameterisations for estragole flux

There are many algorithms for modelling foliar emissions of BVOCs that have been incorporated into models such as MEGAN (Guenther et al., 2006). The potential importance of floral emissions for atmospheric chemistry was recognized by Arey et al. (1991) who report linalool concentrations in an orange tree plantation that are of a similar magnitude to the estragole concentrations observed in this study. However, floral emissions have not been included as a component of regional biogenic emission models due both to the limited quantitative emission rate data and the lack of suitable driving variables. As a result, it is not known what contribution they make to canopy emission. However, oil palms occupy a large land area, and as we showed, the contribution of estragole emissions to total BVOCs can be very high. The actual estragole release and its magnitude are likely to be constrained by biological factors related to the pollination cycle. Because this compound also exhibits deposition, atmospheric models either need to consider this as a loss of part of the emission flux or by including this compound in deposition models. The latter could be derived from the

canopy resistance analogy (Nemitz et al., 2009b; Sutton et al., 1995), and then the overall modelled flux could be represented as in eq. 1:

$$MF = F^+ - V_d(r_a, r_b, r_c) \chi_t(-\Delta\tau) \quad (1)$$

where MF is the modelled flux, $F^+(-\Delta\tau, -\Delta PPF D)$ is the parameterised emission against lag-adjusted ambient temperature (T) and photosynthetic photon flux density ($PPFD$), $V_d(r_a, r_b, r_c)$ is the parameterised deposition velocity, whereas $\chi_t(-\Delta\tau)$ is the empirical volume mixing ratio of estragole estimated empirically from lag-corrected temperature dependence (eq. 2). The lag time for the maximal correlation ($r^2 = 0.40$, $N = 442$) was 3 h.

$$\chi_t = 0.19 \exp(0.1 t_c) \quad (2)$$

In eq. 2, t_c is canopy temperature estimated from resistance approach (eq. 3). Generally t_c was higher by approximately 2-3 °C than t_a (the ambient temperature at the 15 m sensor height) (Fig. 10).

$$t_c = \frac{H (r_a + r_b)}{\rho c_p} + t_a \quad (3)$$

Here H is the sensible heat flux, r_a is the aerodynamic resistance, ρ is air density, and c_p is the specific heat of air.

The equation for emission, F^+ , has been adopted from (Guenther et al., 2006) and modified to include the temperature and PAR lags (eq. 4).

$$F^+ = BER_c \times \mathbf{0.0759} \times \exp(\mathbf{0.02} \times [P_{240} - P_0]) \times [P_{240}]^{0.6} \times [(\mathbf{0.0182} - \mathbf{0.02} \times \ln(P_{240}) \times PPF D / ((1 + (\mathbf{0.0182} - \mathbf{0.02} \times \ln(P_{240}))^2 PPF D^2)^{0.5}))] \times \mathbf{0.71} \times \exp(\mathbf{-0.196} \times (T_{240} - 297)) \times \exp(\mathbf{-0.196} \times (T_{240} - 297)) \times [\mathbf{189} \times \exp(\mathbf{164} \times (4) [(1/(\mathbf{213.5} + (\mathbf{46.09} \times (T_{240} - 297))) + (1/T)) / 0.00831))] / (\mathbf{189} - \mathbf{164} \times (1 - \exp(\mathbf{189} \times [((1/(\mathbf{213.5} + (\mathbf{46.09} \times (T_{240} - 297))) + (1/T)) / 0.00831)])))] \quad (4)$$

The numbers in bold represent the empirical constants that have been parameterised on measurement data of estragole eddy covariance flux at the site. BER_c is canopy-derived basal

emission rate which can be obtained from above equation by substituting F^+ with the eddy covariance flux above canopy (filtered for deposition periods). The correlation of this modelled emission is shown with the measured emission in Fig. 12.

The deposition component of the total parameterised flux contains the deposition velocity (V_d) which can be derived from the resistance approach (eq. 5)

$$V_d(r_a, r_b, r_c) = \frac{1}{r_a + r_b + r_c} \quad (5)$$

where r_b is the laminar boundary layer resistance close to the surface of the leaves, and r_c is the canopy resistance. r_a and r_b were obtained as demonstrated by Nemitz et al. (2009a), and the molecular diffusivity in air D_a for estragole ($6.31 \times 10^{-6} \text{ m}^2 \text{ s}^{-1}$), required in the Schmidt number which is part of the Stanton number which in turn is part of the r_b equation, has been obtained from the molecular structure online calculator (EPA, 2007b) as the average value of WL, FSG and FSG/LaBas estimation methods.

The modelled emission and total flux are intercompared with measured emission in Fig.13. The total average of modelled total flux amounted to $0.22 \text{ mg m}^{-2} \text{ h}^{-1}$ which is only smaller by $0.02 \text{ mg m}^{-2} \text{ h}^{-1}$ from the actual measurement.

It is possible that inflorescences of *E. guineensis* are thermogenic as has been reported for other oil palm species (Knudsen et al., 2001). Thermogenesis presumably helps to volatilise floral scents (in this case estragole) and serves as a cue for pollinators (Ervik et al., 1999). However, although not explicitly tested during this study, thermogenic volatilisation after the decrease in ambient temperature could explain the delayed peak of estragole concentrations with temperature (Terry et al., 2004).

4 Conclusions

The findings of high emissions of estragole from oil palms have important implications for atmospheric chemistry in tropical regions. Using data from this study it is estimated that approximately 300 Gg (10^9 g) of estragole are emitted from oil palm plantations annually. Although almost 3 orders of magnitude less than global isoprene emissions from vegetation,

these estragole emissions are probably the highest single floral contribution of reactive carbon to global atmospheric chemistry. Estragole is present in the aerosol phase as well as the gas phase and is also subject to deposition as well as emission. Since estragole emissions are likely to make a regionally-important contribution to BSOA, whether as an initiator of SOA formation or by being adsorbed on the surface of other particles, the influence on climate is expected to be significant. Although floral emissions are more difficult to model than foliar emissions, we have shown that the latter can also be describable by a Guenther-type algorithm.

A number of uncertainties accompany the above conclusions, including: a comparatively short measurement period; not always the same period of measurement for the different techniques; seasonal variations in emissions; calibration precision; flux errors; and influence of high humidity on measurement sensitivity. Despite these caveats, it is estimated that the overall measurement error should be within a factor of 2 for the PTR-MS concentrations and fluxes, smaller for the in situ GC-MS results, but much larger for data from the enclosures. Clearly, more research is required to understand the mechanisms of estragole formation, its biotic and abiotic controls, and to quantify its emission rates from other tropical species.

Acknowledgements

This work was funded by the UK Natural Environment Research Council (NERC) through the ACES (Aerosol Coupling in the Earth System) project of the APPRAISE (Aerosol Properties PRocesses and InfluenceS on the Earth's climate) research programme. Pawel Misztal thanks his supervisors J. Neil Cape and Mathew R. Heal, and the Centre for Ecology & Hydrology and the School of Chemistry, University of Edinburgh, for funding his PhD. We are grateful to the Sabahmas Plantation, and in particular to Mr. Foo Koh Kei (senior manager) and Mr. Chang Sip Woon (group manager) for the provision of lodging, transport and site infrastructure.

References

- Altshuller, A. P.: REVIEW - NATURAL VOLATILE ORGANIC-SUBSTANCES AND THEIR EFFECT ON AIR-QUALITY IN THE UNITED-STATES, *Atmospheric Environment*, 17, 2131-2165, 1983.
- Binnie, J., Cape, J. N., Mackie, N., and Leith, I. D.: Exchange of organic solvents between the atmosphere and grass - the use of open top chambers, *Science of the Total Environment*, 285, 53-67, 2002.
- Blake, R. S., Monks, P. S., and Ellis, A. M.: Proton-Transfer Reaction Mass Spectrometry, *Chemical Reviews*, 109, 861-896, doi:10.1021/cr800364q, 2009.
- Bouvier-Brown, N. C., Holzinger, R., Palitzsch, K., and Goldstein, A. H.: Quantifying sesquiterpene and oxygenated terpene emissions from live vegetation using solid-phase microextraction fibers, *Journal of Chromatography A*, 1161, 113-120, 2007.
- Bouvier-Brown, N. C., Goldstein, A. H., Worton, D. R., Matross, D. M., Gilman, J. B., Kuster, W. C., Welsh-Bon, D., Warneke, C., de Gouw, J. A., Cahill, T. M., and Holzinger, R.: Methyl chavicol: characterization of its biogenic emission rate, abundance, and oxidation products in the atmosphere, *Atmos. Chem. Phys.*, 9, 2061-2074, 2009a.
- Bouvier-Brown, N. C., Holzinger, R., Palitzsch, K., and Goldstein, A. H.: Large emissions of sesquiterpenes and methyl chavicol quantified from branch enclosure measurements, *Atmospheric Environment*, 43, 389-401, 10.1016/j.atmosenv.2008.08.039, 2009b.
- Buchmann, N., Guehl, J. M., Barigah, T. S., and Ehleringer, J. R.: Interseasonal comparison of CO₂ concentrations, isotopic composition, and carbon dynamics in an Amazonian rainforest (French Guiana), *Oecologia*, 110, 120-131, 1997.
- Chang, C. L., Cho, I. K., and Li, Q. X.: Insecticidal Activity of Basil Oil, trans-Anethole, Estragole, and Linalool to Adult Fruit Flies of *Ceratitis capitata*, *Bactrocera dorsalis*, and *Bactrocera cucurbitae*, *Journal of Economic Entomology*, 102, 203-209, 2009.
- Culf, A. D., Fisch, G., Malhi, Y., Costa, R. C., Nobre, A. D., Marques, A. D., Gash, J. H. C., and Grace, J.: Carbon dioxide measurements in the nocturnal boundary layer over Amazonian forest, *Hydrology and Earth System Sciences*, 3, 39-53, 1999.
- Davison, B., Taipale, R., Langford, B., Misztal, P., Fares, S., Matteucci, G., Loreto, F., Cape, J. N., Rinne, J., and Hewitt, C. N.: Concentrations and fluxes of biogenic volatile organic compounds above a Mediterranean macchia ecosystem in western Italy, *Biogeosciences*, 6, 1655-1670, 2009.
- de Gouw, J., Warneke, C., Karl, T., Eerdeken, G., van der Veen, C., and Fall, R.: Sensitivity and specificity of atmospheric trace gas detection by proton-transfer-reaction mass spectrometry, *International Journal of Mass Spectrometry*, 223-224, 365-382, 2003.
- DeCarlo, P. F., Kimmel, J. R., Trimborn, A., Northway, M. J., Jayne, J. T., Aiken, A. C., Gonin, M., Fuhrer, K., Horvath, T., Docherty, K. S., Worsnop, D. R., and Jimenez, J. L.: Field-deployable, high-resolution, time-of-flight aerosol mass spectrometer, *Analytical Chemistry*, 78, 8281-8289, 10.1021/ac061249n, 2006.
- Test Plan for Estragole: <http://www.epa.gov/HPV/pubs/summaries/estragole/c14022tp.pdf>, access: 21/04/2009, 2002.

U.S. Environmental Protection Agency Estimation Program Interface (EPI) Suite v3.2: <http://www.epa.gov/opptintr/exposure/pubs/episuite.htm>, 2007a.

EPA On-line Tools for Site Assessment Calculation: <http://www.epa.gov/athens/learn2model/part-two/onsite/estdiffusion-ext.htm>, access: 15 Aug 2009, 2007b.

Ervik, F., Tollsten, L., and Knudsen, J. T.: Floral scent chemistry and pollination ecology in phytelephantoid palms (Arecaceae), *Plant Syst. Evol.*, 217, 279-297, 1999.

Foken, T., and Wichura, B.: Tools for quality assessment of surface-based flux measurements, *Agric. For. Meteorol.*, 78, 83-105, 1996.

Geron, C., Owen, S., Guenther, A., Greenberg, J., Rasmussen, R., Hui Bai, J., Li, Q.-J., and Baker, B.: Volatile organic compounds from vegetation in southern Yunnan Province, China: Emission rates and some potential regional implications, *Atmospheric Environment*, 40, 1759-1773, 2006.

Guenther, A., Karl, T., Harley, P., Wiedinmyer, C., Palmer, P. I., and Geron, C.: Estimates of global terrestrial isoprene emissions using MEGAN (Model of Emissions of Gases and Aerosols from Nature), *Atmos. Chem. Phys. Discuss.*, 6, 107-173, 2006.

Hartley, C. W. S.: The oil palm (*Elaeis guineensis* Jacq.), 3rd ed., Tropical Agriculture Series, Longman Scientific & Technical, Harlow, 1988.

Hayes, J. L., and Strom, B. L.: 4-ALLYLANISOLE AS AN INHIBITOR OF BARK BEETLE (COLEOPTERA, SCOLYTIDAE) AGGREGATION, *Journal of Economic Entomology*, 87, 1586-1594, 1994.

Heiden, A. C., Kobel, K., Komenda, M., Koppmann, R., Shao, M., and Wildt, J.: Toluene Emissions from Plants, *Geophys. Res. Lett.*, 26, 1999.

Helmig, D., Ortega, J., Guenther, A., Herrick, J. D., and Geron, C.: Sesquiterpene emissions from loblolly pine and their potential contribution to biogenic aerosol formation in the Southeastern US, *Atmospheric Environment*, 40, 4150-4157, 2006.

Hewitt, C. N., Lee, J., Barkley, M. P., Carslaw, N., Chappell, N. A., Coe, H., Collier, C., Commane, R., Davies, F., DiCarlo, P., Di Marco, C. F., Edwards, P. M., Evans, M. J., Fowler, D., Furneaux, K. L., Gallagher, M., Guenther, A., Heard, D. E., Helfter, C., Hopkins, J., Ingham, T., Irwin, M., Jones, C., Karunaharan, A., Langford, B., Lewis, A. C., Lim, S. F., MacDonald, S. M., MacKenzie, A. R., Mahajan, A. S., Malpass, S., McFiggans, G., Mills, G., Misztal, P., Moller, S., Monks, P. S., Nemitz, E., Nicolas-Perea, V., Oetjen, H., Oram, D., Palmer, P. I., Phillips, G. J., Plane, J. M. C., Pugh, T., Pyle, J. A., Reeves, C. E., Robinson, N. H., Stewart, D., Stone, D., and Whalley, L. K.: Oxidant and particle photochemical processes above a south-east Asian tropical rain forest (the OP3 project): introduction, rationale, location characteristics and tools, *Atmos. Chem. Phys. Discuss.*, 9, 18899-18963, 2009.

Holzinger, R., Lee, A., Paw, K. T., and Goldstein, A. H.: Observations of oxidation products above a forest imply biogenic emissions of very reactive compounds, *Atmospheric Chemistry and Physics*, 5, 67-75, 2005.

Hussein, M. Y., Lajis, N. H., Kinson, A., and Teo, C. B.: Laboratory and field evaluation on the attractancy of *Elaeidobius kamerunicus* Faust to 4-allylanisole, *Porim Bull.*, 18, 20-26, 1989.

- Hussein, M. Y., Lajis, N. H., and Ali, J. H.: Biological and chemical factors associated with the successful introduction of *Elaeidobius kamerunicus* Faust, the oil palm pollinator in Malaysia, *Acta Hort. (ISHS)* 288, 81-87, 1991.
- Jayne, J. T., Leard, D. C., Zhang, X. F., Davidovits, P., Smith, K. A., Kolb, C. E., and Worsnop, D. R.: Development of an aerosol mass spectrometer for size and composition analysis of submicron particles, *Aerosol Science and Technology*, 33, 49-70, 2000.
- Jimenez, J. L., Jayne, J. T., Shi, Q., Kolb, C. E., Worsnop, D. R., Yourshaw, I., Seinfeld, J. H., Flagan, R. C., Zhang, X. F., Smith, K. A., Morris, J. W., and Davidovits, P.: Ambient aerosol sampling using the Aerodyne Aerosol Mass Spectrometer, *J. Geophys. Res.-Atmos.*, 108, 8425
10.1029/2001jd001213, 2003.
- Karl, T. G., Spirig, C., Rinne, J., Stroud, C., Prevost, P., Greenberg, J., Fall, R., and Guenther, A.: Virtual disjunct eddy covariance measurements of organic compound fluxes from a subalpine forest using proton transfer reaction mass spectrometry, *Atmospheric Chemistry and Physics*, 2, 279-291, 2002.
- Kim, S., Karl, T., Helmig, D., Daly, R., Rasmussen, R., and Guenther, A.: Measurement of atmospheric sesquiterpenes by proton transfer reaction-mass spectrometry (PTR-MS), *Atmos. Meas. Tech. Discuss.*, 1, 401-433, 2008.
- Knudsen, J. T., Tollsten, L., and Ervik, F.: Flower scent and pollination in selected neotropical palms, *Plant Biology*, 3, 642-653, 2001.
- Langford, B., Davison, B., Nemitz, E., and Hewitt, C. N.: Mixing ratios and eddy covariance flux measurements of volatile organic compounds from an urban canopy (Manchester, UK), *Atmos. Chem. Phys.*, 9, 1971-1987, 2009.
- Lee, A., Goldstein, A. H., Keywood, M. D., Gao, S., Varutbangkul, V., Bahreini, R., Ng, N. L., Flagan, R. C., and Seinfeld, J. H.: Gas-phase products and secondary aerosol yields from the ozonolysis of ten different terpenes, *J. Geophys. Res.-Atmos.*, 111, 10.1029/2005jd006437, 2006a.
- Lee, A., Goldstein, A. H., Kroll, J. H., Ng, N. L., Varutbangkul, V., Flagan, R. C., and Seinfeld, J. H.: Gas-phase products and secondary aerosol yields from the photooxidation of 16 different terpenes, *J. Geophys. Res.-Atmos.*, 111, 10.1029/2006jd007050, 2006b.
- Lindinger, W., Hansel, A., and Jordan, A.: On-line monitoring of volatile organic compounds at pptv levels by means of proton-transfer-reaction mass spectrometry (PTR-MS) - Medical applications, food control and environmental research, *International Journal of Mass Spectrometry*, 173, 191-241, 1998.
- Mahbob, A.: The Pollinator *E. Camerunicus* is Nature's little helper, *Global Oil & Fats Business Magazine*, 5, 58-59, 2008.
- Moura, J. I. L., Cividanes, F. J., dos Santos, L. P., and Valle, R. R.: Pollination of oil palm by weevils in Southern Bahia, Brazil, *Pesquisa Agropecuaria Brasileira*, 43, 289-294, 2008.
- Nemitz, E., Hargreaves, K. J., Neftel, A., Loubet, B., Cellier, P., Dorsey, J. R., Flynn, M., Hensen, A., Weidinger, T., Meszaros, R., Horvath, L., D mmgen, U., Fr hauf, C., L pmeier, F. J., Gallagher, M. W., and Sutton, M. A.: Intercomparison and assessment of turbulent and physiological exchange parameters of grassland, *Biogeosciences*, 6, 1445-1466, 2009a.

- Nemitz, E., Loubet, B., Lehmann, B. E., Cellier, P., Neftel, A., Jones, S. K., Hensen, A., Ihly, B., Tarakanov, S. V., and Sutton, M. A.: Turbulence characteristics in grassland canopies and implications for tracer transport, *Biogeosciences*, 6, 1519-1537, 2009b.
- Rinne, H. J. I. G., A. B.; Warneke, C.; de Gouw, J. A.; Luxembourg, S. L.: Disjunct eddy covariance technique for trace gas flux measurements, *Geophysical Research Letters*, 28, 3139-3142, 2001.
- Rinne, J., Taipale, R., Markkanen, T., Ruuskanen, T. M., Hellm n, H., Kajos, M. K., Vesala, T., and Kulmala, M.: Hydrocarbon fluxes above a Scots pine forest canopy: measurements and modeling, *Atmos. Chem. Phys.*, 7, 3361-3372, 2007.
- Rosenstiel, T. N., Potosnak, M. J., Griffin, K. L., Fall, R., and Monson, R. K.: Increased CO₂ uncouples growth from isoprene emission in an agriforest ecosystem, *Nature*, 421, 256-259, 10.1038/nature01312, 2003.
- Spirig, C., Neftel, A., Ammann, C., Dommen, J., Grabmer, W., Thielmann, A., Schaub, A., Beauchamp, J., Wisthaler, A., and Hansel, A.: Eddy covariance flux measurements of biogenic VOCs during ECHO 2003 using proton transfer reaction mass spectrometry, *Atmospheric Chemistry and Physics*, 5, 465-481, 2005.
- Steinbacher, M., Dommen, J., Ammann, C., Spirig, C., Neftel, A., and Prevot, A. S. H.: Performance characteristics of a proton-transfer-reaction mass spectrometer (PTR-MS) derived from laboratory and field measurements, *International Journal of Mass Spectrometry*, 239, 117-128, 2004.
- Sutton, M. A., Burkhardt, J. K., Guerin, D., Nemitz, E., and Fowler, D.: Development of resistance models to describe measurements of bi-directional ammonia surface-atmosphere exchange, *International Conference on Atmospheric Ammonia - Emissions, Deposition and Environmental Impacts*, Culham, England, 1995, ISI:000072633600029, 473-480,
- Syed, R. A.: Studies on oil palm pollination by insects, *Bull. ent. Rev.*, 69, 1979.
- Taipale, R., Ruuskanen, T. M., Rinne, J., Kajos, M. K., Hakola, H., Pohja, T., and Kulmala, M.: Technical Note: Quantitative long-term measurements of VOC concentrations by PTR-MS - measurement, calibration, and volume mixing ratio calculation methods, *Atmospheric Chemistry and Physics*, 8, 6681-6698, 2008.
- Terry, I., Moore, C. J., Walter, G. H., Forster, P. I., Roemer, R. B., Donaldson, J. D., and Machin, P. J.: Association of cone thermogenesis and volatiles with pollinator specificity in *Macrozamia* cycads, *Plant Syst. Evol.*, 243, 233-247, 10.1007/s00606-003-0087-x, 2004.
- Wahid, M. B., and Kamarudin, N. H. J.: Role and effectiveness of *Elaeidobius kamerunicus*, *Thrips hawaiiensis*, and *Pyroderces* sp. in pollination of mature oil palm in peninsular Malaysia, *Elaeis*, 9, 1-16, 1997.
- Wang, Y. F., Owen, S. M., Li, Q. J., and Penuelas, J.: Monoterpene emissions from rubber trees (*Hevea brasiliensis*) in a changing landscape and climate: chemical speciation and environmental control, *Glob. Change Biol.*, 13, 2270-2282, 2007.

Table 1. Intercomparison of estragole volume mixing ratios (have I left out any numbers?)

Site/ date / source	PTR-MS (ambient 15 m)	GC-MS (flower enclosure)	GC-MS (ambient)	GC-MS (leaf)	PTR-MS/TA above
Borneo (Oil palm) / 29-05-2008 – 11/06/2008 / this work	3.0 ^a ppbv				
Borneo (Oil palm) / 25-05-2008 / this work			1.2 ppb (morning 9:00 to 10:00) 3.0 ppb (early afternoon 12:00 to 14:00) 3.8 ppb (late afternoon 14:00 to 16:00)	< 0.2 ppbv	
Blodget Forest (ponderosa pine)/ (Bouvier-Brown et al., 2009a; Bouvier-Brown et al., 2009b)					few pp
Borneo (Oil palm)/ 15/5/2009 – 17/5/2009 / this work		Female flowers ~0.26–1.39 ppm ^d (60 ppm ^e) Male flowers ~ 150 ppb ^f			

^amean over the measurement period (N=537) ^bmorning ^cafternoon (16:00); ^caccumulated in the enclosure (~ 3L airspace) for an hour; ^daccumulated in the enclosure (~2L headspace); ^eit might be possible that the tube touched the flower;

Table 2 Intercomparison of estragole fluxes

Site/ date / source	PTR-MS vDEC (ambient 15 m)	GC-MS (flowers)	GC-MS (fronds)	GC-FID and PTR-MS (branch level)
Borneo (Oil palm) / 29-05-2008 – 11/06/2008 / this work	0.49 ^a mg m ⁻² h ⁻¹ 0.24 ^b mg m ⁻² h ⁻¹			
Borneo (Oil palm) / 25-05-2008 / this work			~ 1 µg g ⁻¹ h ⁻¹	
Blodget Forest (ponderosa pine)/ (Bouvier-Brown et al., 2009b)				0.20 ^c mg m ⁻² h ⁻¹

Borneo (Oil palm)/ 15/52009 – 17/5/2009 / this work		Female flowers ~ 0.03 mg m ⁻² h ⁻¹ ^d		
--	--	--	--	--

^amid-day mean 10:00 – 14:00 (N = 80); ^b24-h average of 12 days (N =584) ^cderived from basal rate of 1.37 μmol m⁻² hr⁻¹ (Bouvier-Brown et al., 2009a); ^dexpected to be considerably underestimated (explanation in section 3.4)

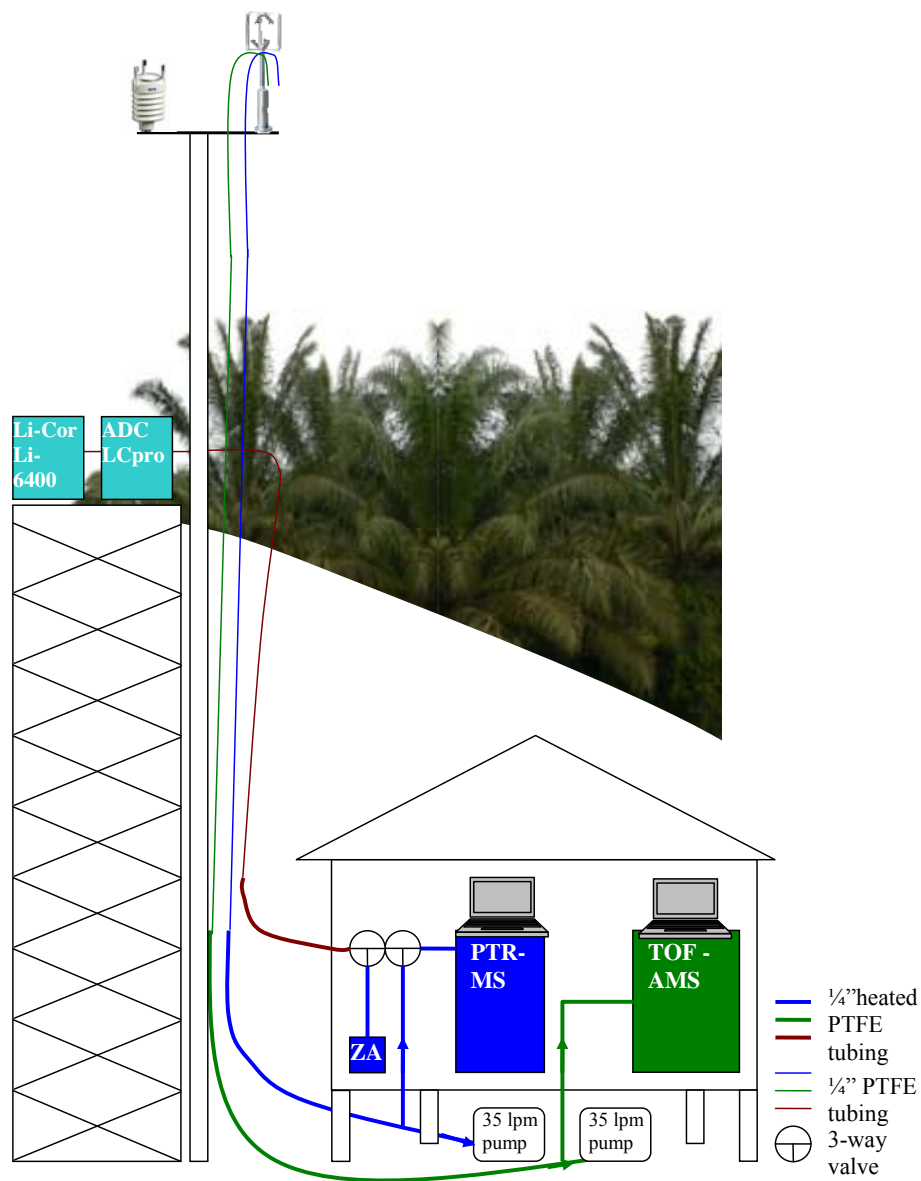


Figure 1. Schematic of the set-up.

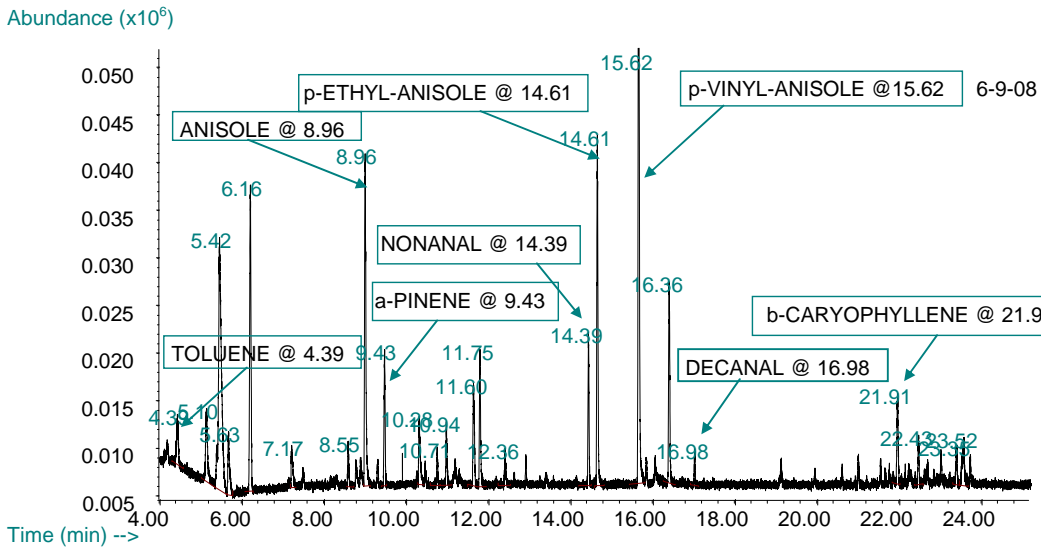


Figure 2. The chromatogram of air from an old fig (*Ficus* spp.) tree leaf in the Borneo rainforest, showing a range of anisoles but not p-allyl-anisole (estragole).

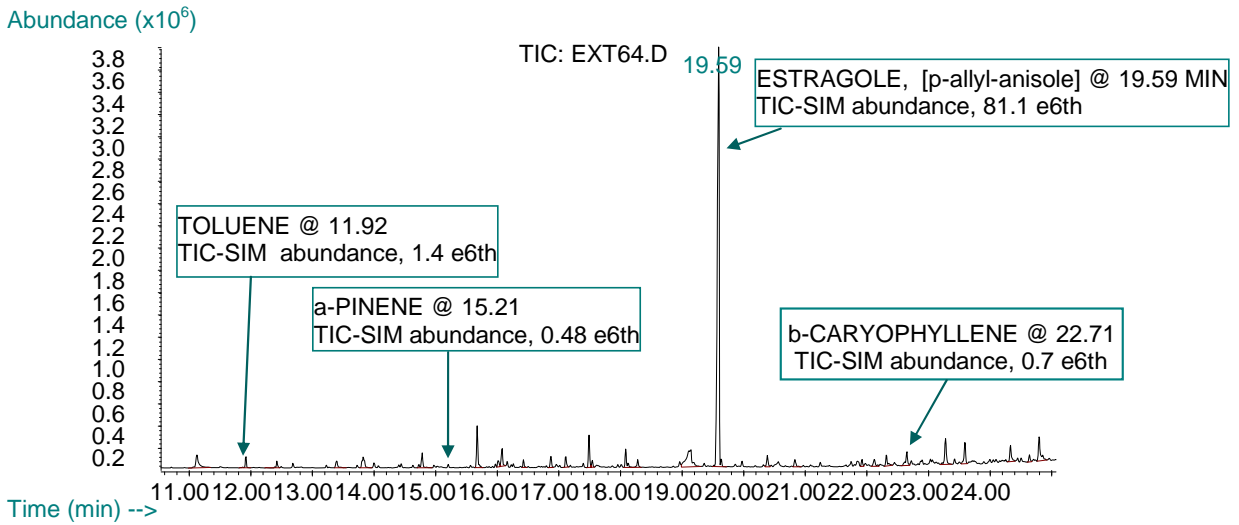


Figure 3. Chromatogram of ambient air sampled within the oil palm canopy, showing a high abundance of estragole (p-allyl-anisole) but not of any of its derivatives. Oil palm plantation ambient air at ground level sampled on 25th May 2008. 15 m/z ions monitored

Comment [PKM3]: What was the retention time of isoprene?

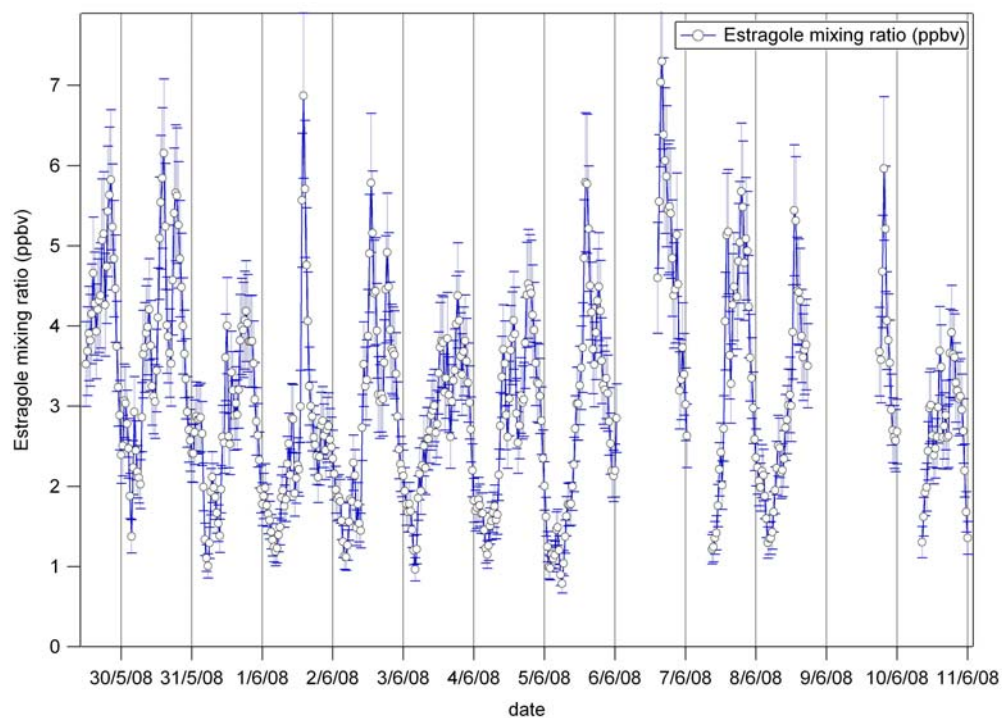
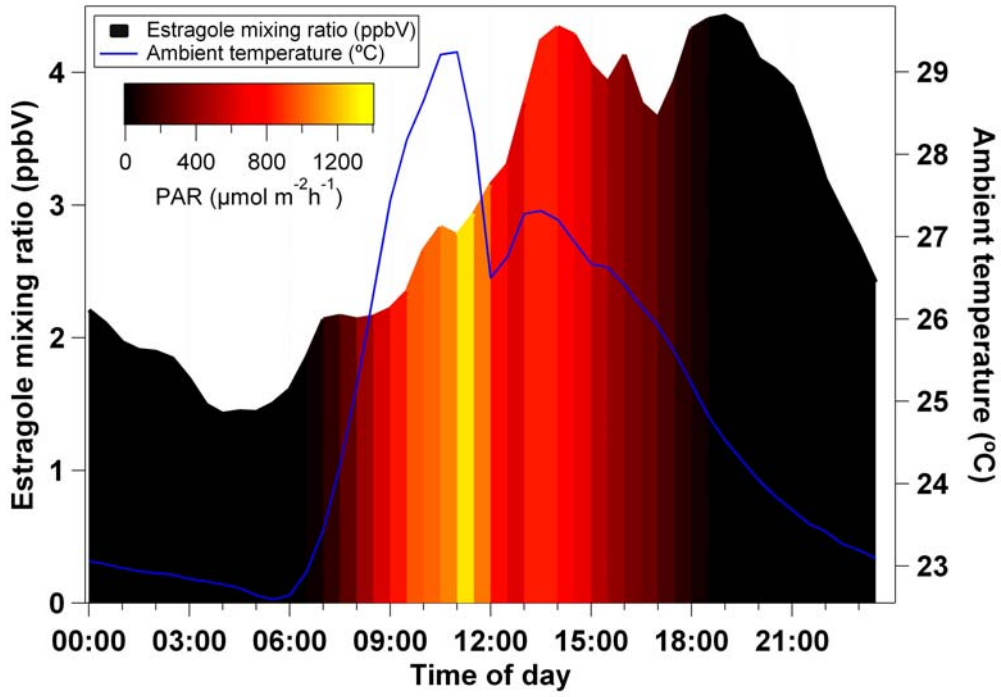


Figure 4. Time-series of volume mixing ratios (ppbv) of estragole measured by PTR-MS above the oil palm canopy.

a)



b)

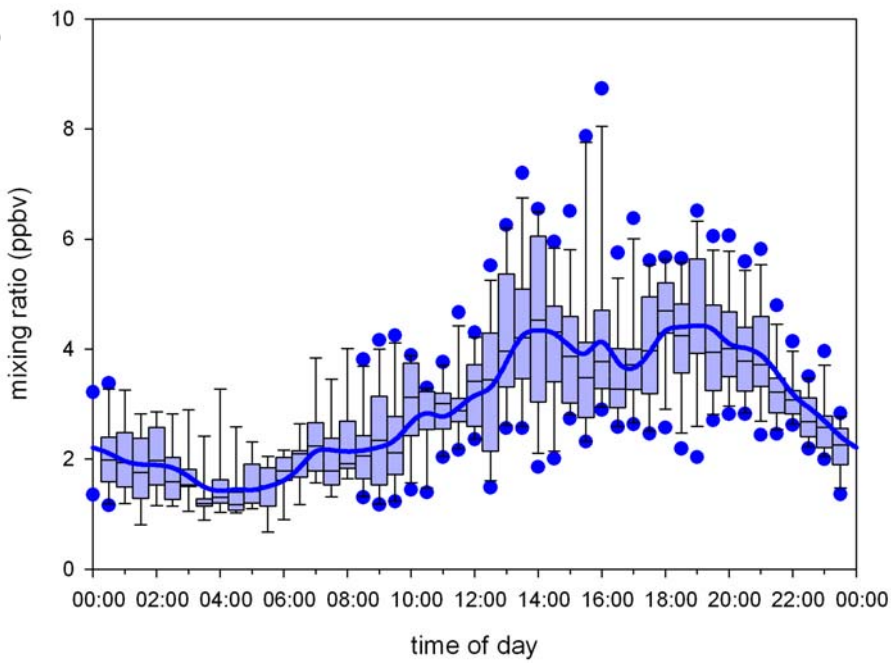


Figure 5. Diurnal graphs of estragole mixing ratios (left axis): a) in relation to temperature (right axis) and PAR (grey scale); b) Box-and-Whisker plot of day-to-day variability.

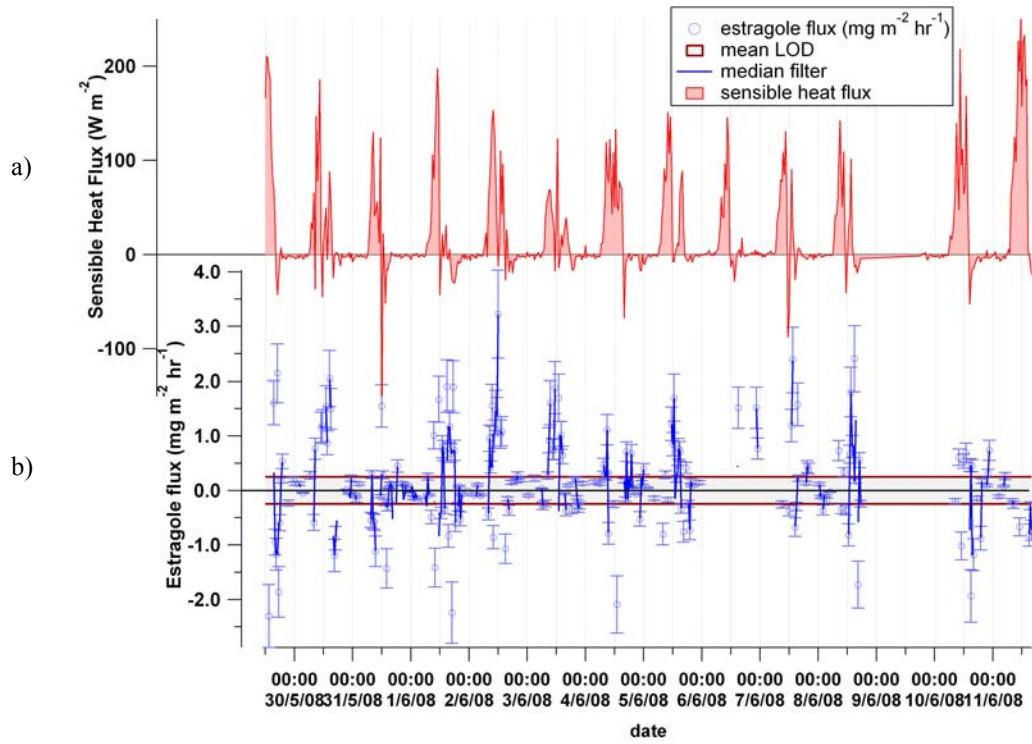


Figure 6. (a) Sensible heat flux and (b) estragole flux with uncertainty bars, running median, and limit of detection (LOD).

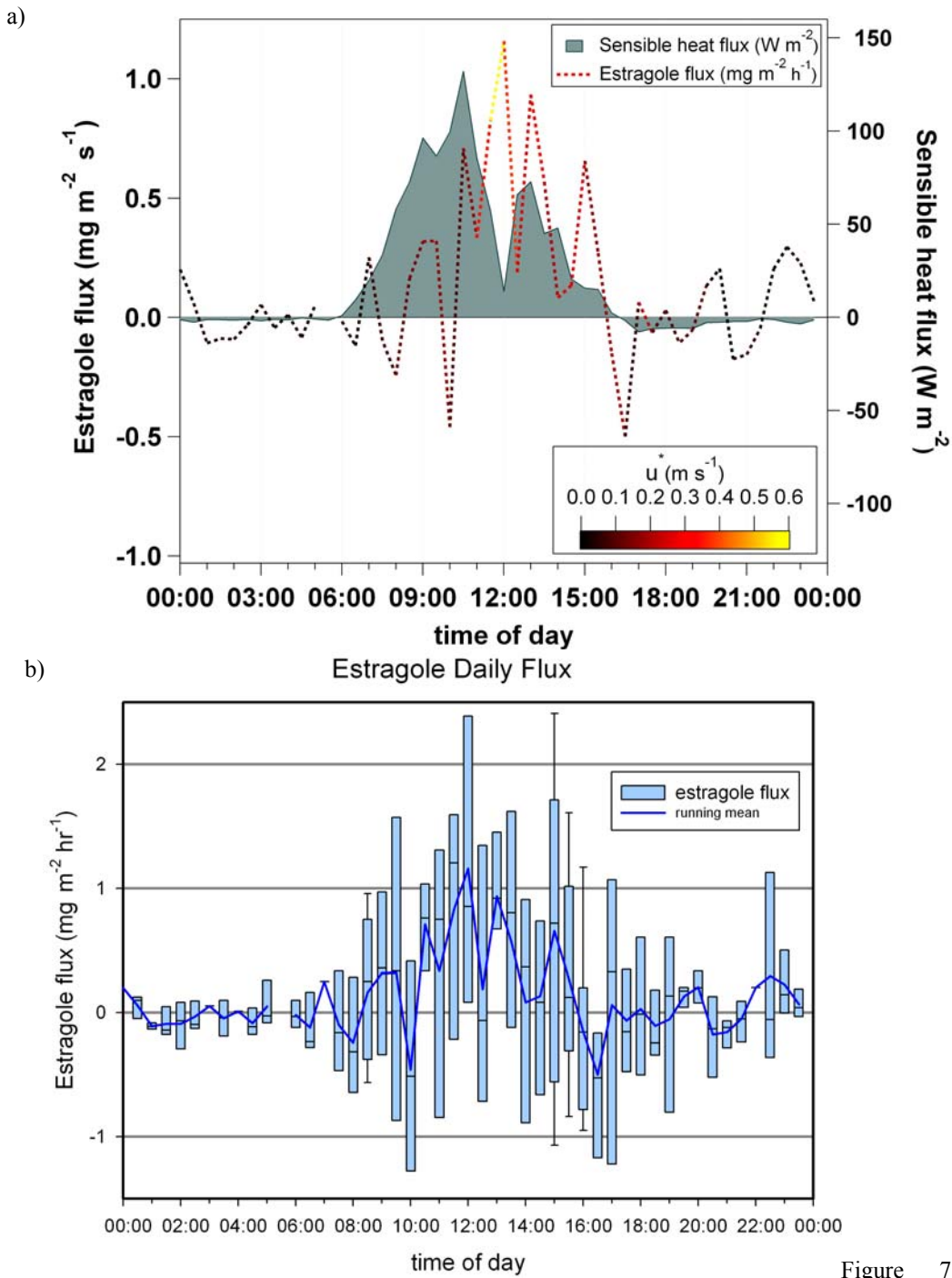


Figure 7.

Average diurnal cycles of the estragole flux: a) Box-and-Whisker plots showing day-to-day variability; b) in comparison with sensible heat flux (right axis), and shaded by u^* .

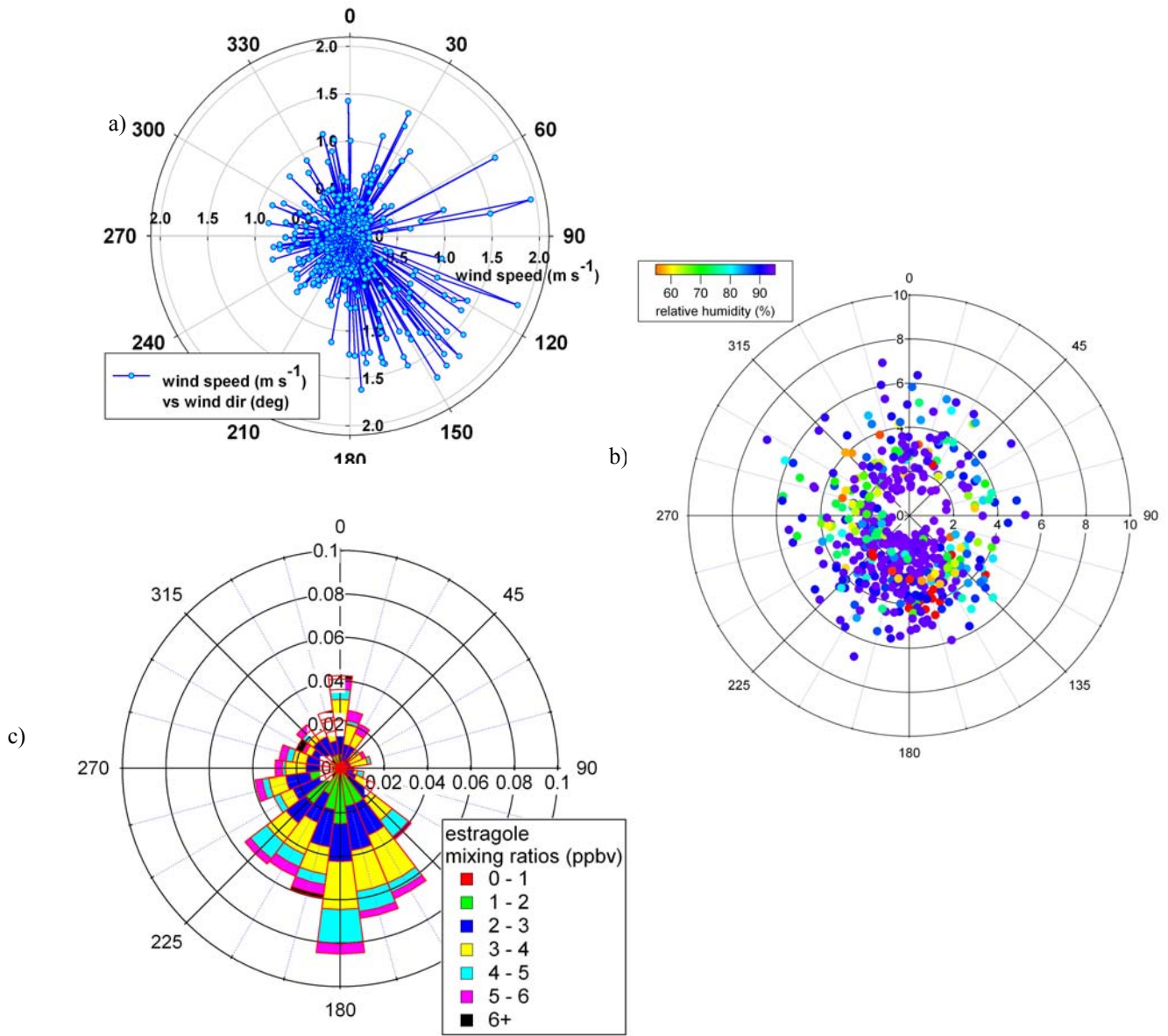


Figure 8. a) polar plot of wind direction and wind speed. b) Polar plot of estragole mixing ratios (ppbV) – radial axes, vs wind direction (deg) – angular axis, coloured in dependence on relative humidity. c) Wind rose plot of estragole mixing ratios (probability 0-1 on radial axes).

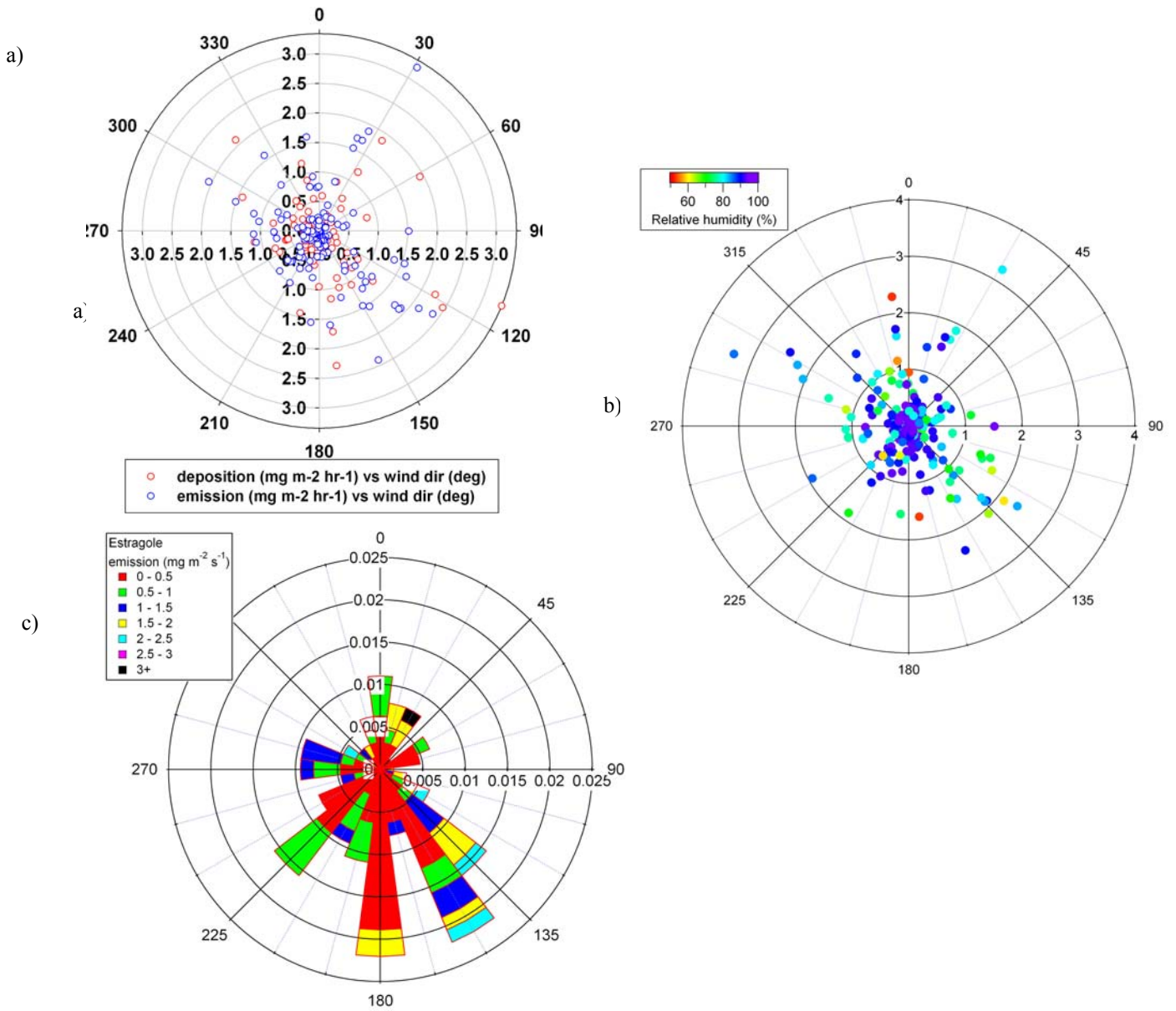


Figure 9. a) polar plot of emission and deposition of estragole; b) polar plot of estragole emission ($\text{mg m}^{-2} \text{h}^{-1}$) vs wind direction (deg) coloured by RH (%); c) Wind rose of estragole emission (probability on radial axis).

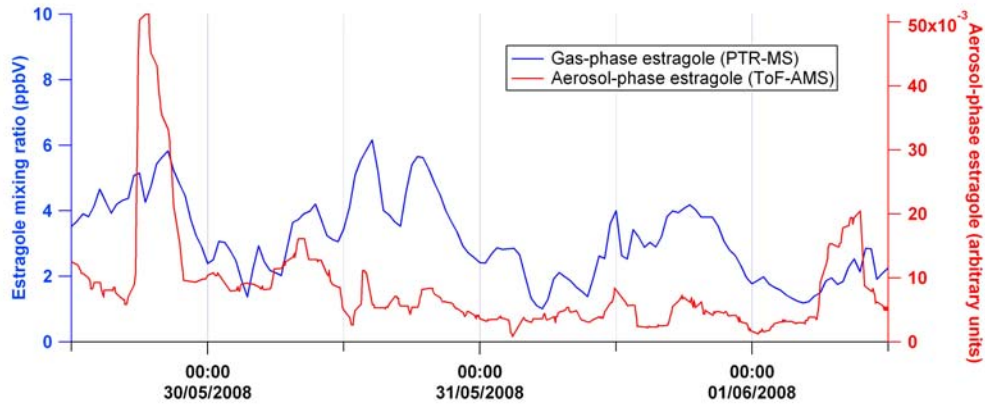


Fig 10. Estragole in gas phase as measured by PTR-MS (blue) and in the aerosol phase (measured by AMS) as estimated from typical fragmentation patterns for estragole.

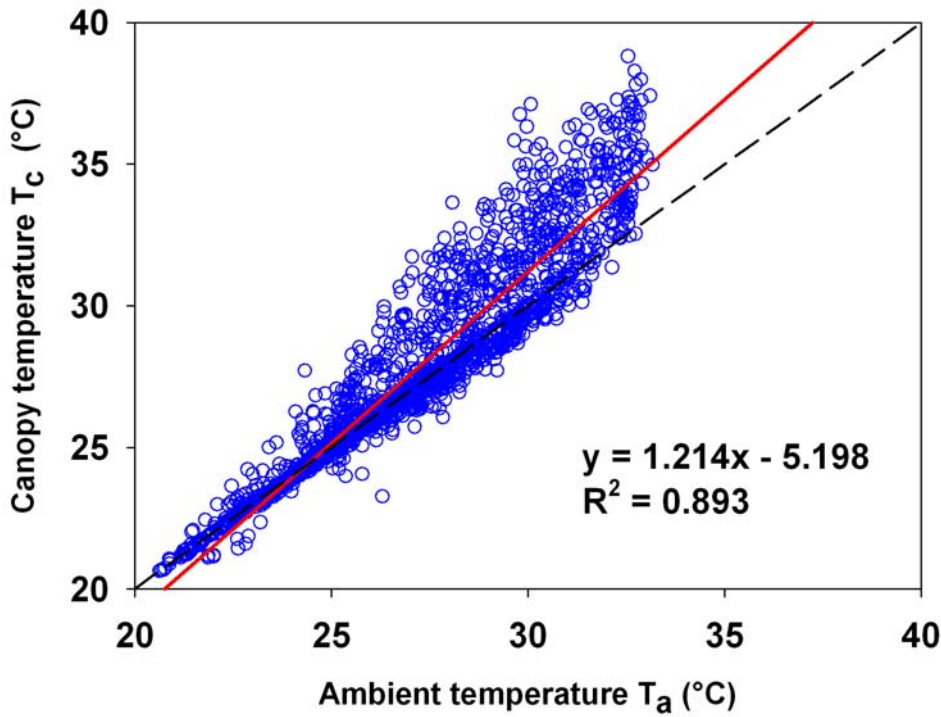


Fig. 11. Measured temperature 3 metres above canopy (t_a) intercompared with canopy temperature (t_c) estimated from the resistance approach. Dash line denotes 1:1 slope.

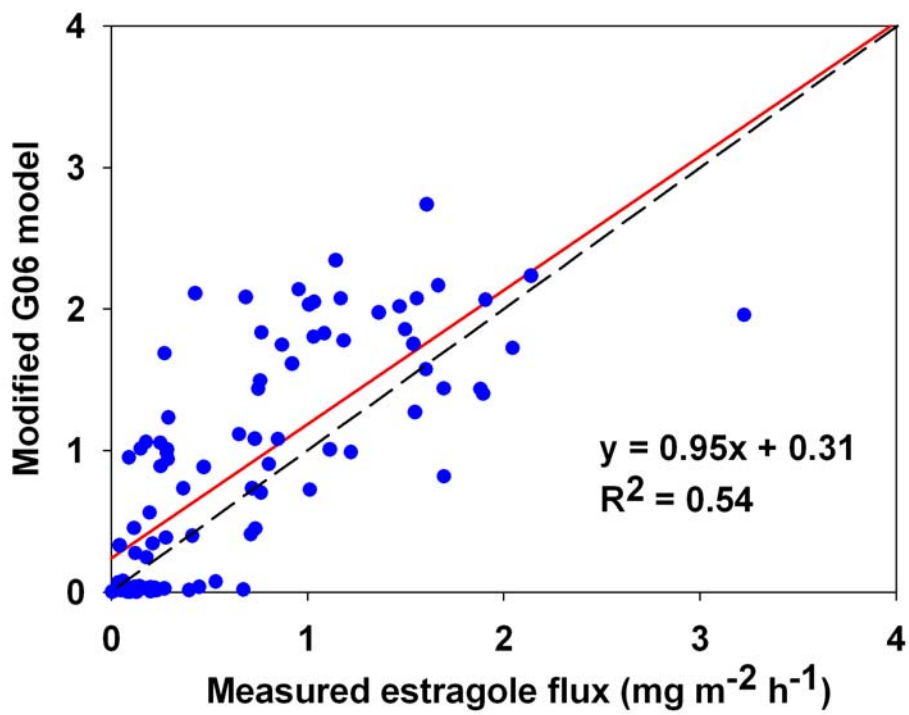


Fig 11. Measured estragole fluxes (positive values only) plotted against the optimised model (G06) for estragole emissions.

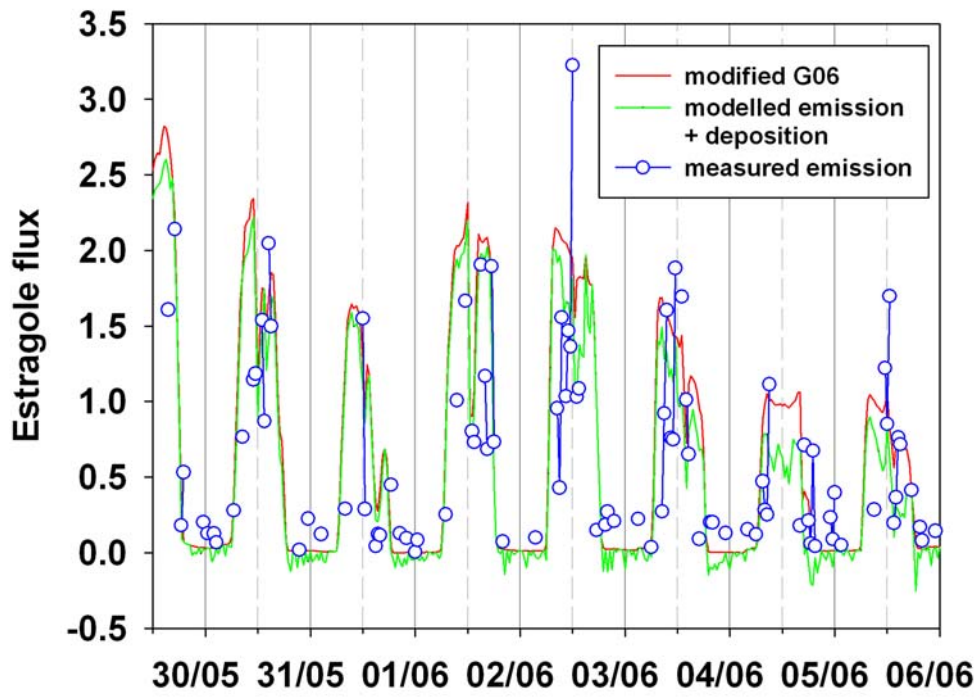


Fig. 12. Timeseries of measured estragole flux (values filtered for emission) in relation to modelled emission by modified G06 and total modelled flux (incl. deposition).